Polymer 50 (2009) 591–597

Contents lists available at ScienceDirect

Polymer

journal homepage: www.elsevier.com/locate/polymer

Fatigue testing of implantable specimens: Effect of sample size and branching on the dynamic fatigue properties of polyisobutylene-based biomaterials

Judit E. Puskas [a,*], Lucas M. Dos Santos [a], Frank Fischer [b], Christian Götz [b], Miroslawa El Fray [c], Volker Altstädt [b], Matthew Tomkins [d]

[a] Department of Polymer Science, The University of Akron, Goodyear Polymer Center, Room 420, 170 University Ave., Akron, OH 44325-3909, USA
[b] Department of Polymer Engineering, University of Bayreuth, Universitätstr, 30, 95447 Bayreuth, Germany
[c] Division of Biomaterials and Microbiological Technologies, Polymer Institute, Szczecin University of Technology, Pulaskiego 10, Szczecin 70-322, Poland
[d] Department of Chemical Engineering, The University of Western Ontario, London, ON, Canada

ARTICLE INFO

Article history:
Received 31 July 2008
Received in revised form
28 October 2008
Accepted 31 October 2008
Available online 30 November 2008

Keywords:
Poly(styrene-*b*-isobutylene-*b*-styrene) SIBS
Long chain branching
In vitro tensile testing

ABSTRACT

In this paper we present the first results on the effect of specimen size and branching on the fatigue properties of polyisobutylene-based thermoplastic elastomers measured by the hysteresis method. It was verified that smaller specimens were inherently stronger as expected; at the same loading rate microdumbbells induced higher strain rates so they can be considered as the "worst case" scenario. Microdumbbells, which can be implanted into small animals for in vivo studies, were used for dynamic fatigue testing of linear poly(styrene-*b*-isobutylene-*b*-styrene) triblock copolymers (L_SIBS) in comparison with long-chain branched (tree-like or dendritic) versions (D_SIBS). In dynamic stress relaxation studies, D_SIBS performed better than L_SIBS. Simulated physiological conditions had negligible effect on the dynamic properties.

© 2008 Elsevier Ltd. All rights reserved.

1. Introduction

Linear triblock poly(styrene-*b*-isobutylene-*b*-styrene) (SIBS) copolymers made by living carbocationic polymerization that exhibited good thermoplastic elastomeric (TPE) properties were introduced in the early 1990s [1–3]. Since the FDA approval of the Taxus drug eluting coronary stent in 2004, SIBS has been used in clinical practice as the coating on the stent under the trade name of Translute™ [4,5]. SIBS is biocompatible in ultra-long term endoluminal (vascular) device applications and more stable than stents coated with medical-grade polyurethanes (PUs) [6]. SIBS is transparent and resembles medical-grade silicone rubber, but does not need reinforcing fillers or chemical crosslinkers on account of its capability to self-assemble into a thermo-labile network structure. We have found that in addition to good hemo- and biocompatibility, SIBS had better fatigue properties in air and in vitro than medical-grade silicone [7].

The third generation of SIBS with an *arborescent* (long-chain branched, tree-like and often called hyperbranched or dendritic) polyisobutylene (PIB) core blocked with polystyrene (PS) (D_SIBS, see Fig. 1) was found to have a unique combination of properties [8–12]. Encrustation of D_SIBS in a rabbit model was found to be comparable or better than that of medical-grade silicone rubber [13]. Hemolysis and 30- and 180-day implantation studies revealed excellent biocompatibility of this emerging biomaterial [7].

Given the increasing number of applications of polymeric biomaterials, establishing reliable methods for evaluating their short and long term mechanical and fatigue properties, as well as their performance under physiological conditions in the body is a subject of great importance.

We have reported that the dynamic fatigue properties of SIBS with 30 wt% PS (SIBS30), tested by the hysteresis method adopted for biomaterials [15–17], are between polyurethane and silicone rubber, with twice as long fatigue life as silicone [7]. Under Single Load Testing (SLT, 1.25 MPa) SIBS30 displayed less than half the dynamic creep compared to silicone, both in air and in vitro (37 °C, simulated body fluid). In this journal we will also show (the two papers are submitted together, the other one was already accepted, reference: JPOL 12810) that SIBS also compared well with polyester and polyurethane biomaterials under strain-controlled testing [18].

In this paper we present the first results on the effect of specimen size and branching on the stress relaxation of PIB-based TPE biomaterials.

* Corresponding author. Tel.: +1 330 972 6203; fax: +1 330 972 5290.
E-mail address: jpuskas@uakron.edu (J.E. Puskas).

0032-3861/$ – see front matter © 2008 Elsevier Ltd. All rights reserved.
doi:10.1016/j.polymer.2008.10.061

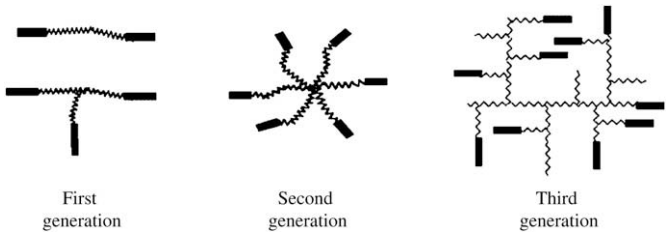

Fig. 1. Three generations of PIB-based TPEs [14].

2. Materials and methods

2.1. Materials

Semi-commercial SIBS samples under the trade name of SIBSTAR (SIBS073T and SIBS103T density = 0.954 g/cm^3, PS content = 31 and 34 wt%, melt flow rate = 7 g/10 min and 1 g/10 min (230 °C, 2.16 kg) respectively) was obtained courtesy of Kaneka Corp., Osaka, Japan. These linear SIBS samples are designated L_SIBS31 and L_SIBS34, respectively. *Arborescent* (dendritic) SIBS, having 16 and 33 wt% PS, designated D_SIBS16 and D_SIBS33 respectively, were synthesized as reported [19]. Characteristic data are summarized in Table 1. The average number of branches per chain B is 2.1 for D_SIBS33 and 1.3 for D_SIBS16.

Simulated body fluid (SBF) was prepared by adding reagent grade chemicals to 8.8 L of distilled water to obtain ion concentrations (Na^+, K^+, NH_4^+, Mg^{2+}, Ca^{2+}, Cl^-, HCO_3^-, HPO_4^{2-} and SO_4^{2-}) found in the human body: NaCl (55.4 g), $NaHCO_3$ (21.47 g), $MgCl_26H_2O$ (1.79 g), Na_2SO_4 (0.0044 g), $NaNH_4HPO_4$ (1.43 g), KCl (3.29 g), $CaCl_2$ (1.29 g). All chemicals were obtained from Aldrich, Germany. The SBF was buffered with tris-hydroxymethyl aminomethane to a pH of 7.4 to mimic physiological conditions [20–22]. pH was measured by Hanna Instruments HI 8314 membrane pH meter.

2.2. Sample preparation

Samples were first compression molded and subsequently die-cut to the appropriate standard specimen sizes (ASTM D412-98a: standard sized dumbbells and ASTM D 1708-02a: microdumbbells). Fig. 2 shows the dumbbell shape and the respective sizes are shown in Table 2. The press was pre-heated to 150 °C, the polymer samples were added and pre-heated for 5 min at this temperature and then pressed at 170 MPa for 3 min. The sheets were then allowed to cool and removed from the press once they reached room temperature.

2.3. Tensile testing

A Zwick Z020 universal testing machine equipped with a 100 N load cell was used to obtain tensile data. Data were collected by test Xpert V.8.1 software. 500 mm/min speed was used for the determination of the ultimate tensile strength (UTS, σ) and ultimate elongation (ε), in accordance with ASTM and the German DIN 53 455 standard for tensile testing. Tests were completed in a climate controlled room with an air temperature of 24 °C, and in SBF at 24 °C and at 37 °C, using an environmental chamber of sufficient size surrounding the sample and the testing arm throughout the entire runs as reported earlier [7]. The chamber was attached to the testing head in a way that it did not interfere with the static cross-head during the experiments. The environmental chamber was charged with SBF to the necessary level to completely immerse the samples. A combined pump and heating unit equipped with a thermocouple was used to accurately control the temperature. Final results were averaged over 5 specimens.

Table 1
Characteristic data of linear and dendritic SIBS [7,19].

Material	M_n (g/mol)	M_w/M_n	σ^a (MPa)	ε^b (%)	Shore A hardness
L-SIBS31	67,000	1.24	13.1	440	40
L-SIBS34	78,000	1.70	15.0	600	54
D-SIBS16	119,000	2.41	6.3	900	22
D-SIBS33	70,000	4.45	5.8	490	41

500 mm/min cross-head speed (ASTM D412 and DIN 53 455). Average of 5 measurements; typical SD = 0.1 MPa and 20%.
[a] σ = stress at break.
[b] ε = elongation at break.

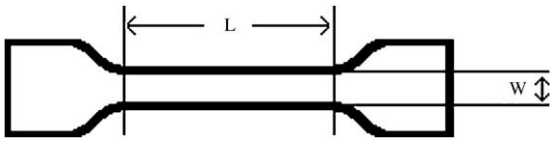

Fig. 2. Dumbbell-shaped tensile specimens.

2.4. Fatigue testing

A servo-hydraulic test machine (Instron 8800) equipped with a digital controller and DynMat custom software package (BASF) was used as described in previous papers [15,16]. Air temperature was controlled and kept constant at 24 °C. A 100 N Kraftaufnehmer KAF-S load cell was bolted to the cross-head in order to measure instantaneous forces on the polymer as a function of time. Strain was measured as the displacement of the moving head from the clamp. The fatigue limit was determined using a Stepwise Increasing Strain Test (SIST). In order to avoid buckling, maximum strain and minimum stress were controlled. During SIST testing, the sample was subjected to a cyclic deformation at a constant frequency of 1 Hz. Strains started at 10–15% and were increased by 5% increments up to a maximum of 55%. Between each step, 100 cycles were allowed for the system to reach the next plateau. The clamp distance was set to 25 mm for microdumbbells and 40 mm for the standard dumbbell samples. The dynamic modulus (E_{dyn}) was tracked in each step in the SIST. Data were collected every 10 s while increases in stress were limited to 0.1 N/mm^2 over a single cycle by the software, due to the softness of the material.

Long term tests (100,000 cycles) were conducted with the measured fatigue limit strain of each material, in air at 24 °C. Tests in SBF were conducted by first recording 12,000 cycles (3 h and 20 min) in air at 24 °C in order to provide a baseline, followed by 12,000 cycles in SBF at 37 °C to mimic physiological conditions.

3. Results and discussion

3.1. Comparison of standard dumbbells and microdumbbells

During our continued testing of biomaterials, we realized that it would be important to develop a fatigue testing methodology for small specimens (microdumbbells) that can be implanted into small animals and re-tested after explantation. Virtually all scientific literature concerning new biomaterials uses microdumbbells for testing because of limited sample availability. The size dependence of mechanical properties is well documented in the mechanics literature [23–26]. According to Weibull [26] the statistical distribution of flaws is inversely proportional to size. This

Table 2
Dumbbell specimen sizes.

Shape name	L (mm)	W (mm)	Thickness (mm)	Cross-sectional area (mm^2)
Standard	40	6.2	2.3	14.26
Micro	25	2.6	1.0	2.60

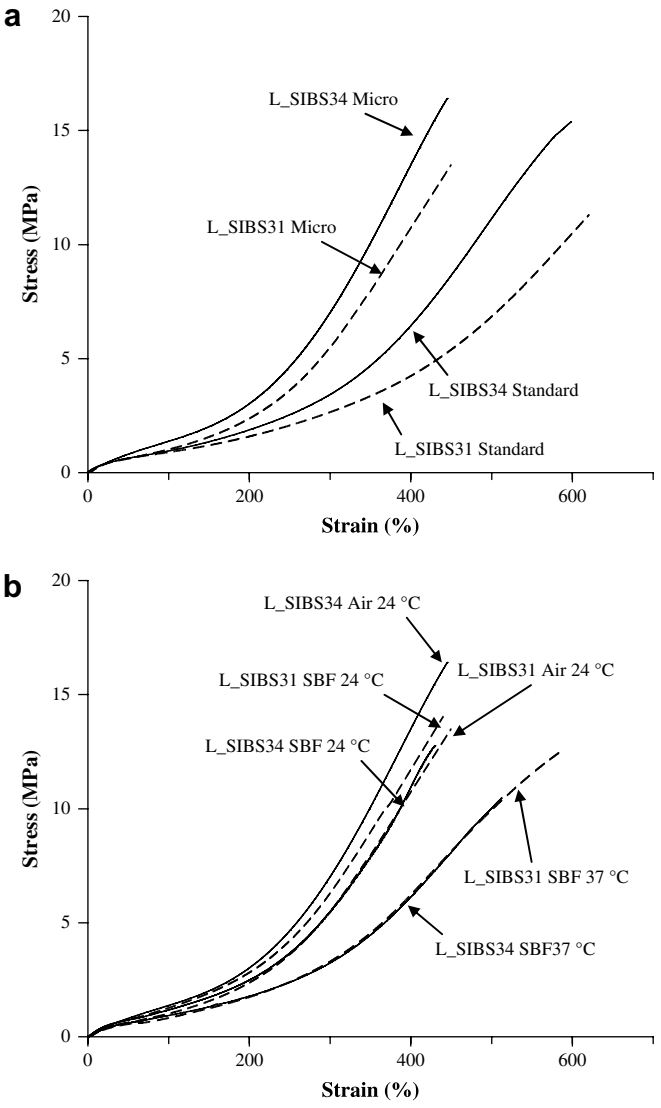

Fig. 3. Stress–strain plots of L_SIBS. (a) Comparison of standard and microdumbbells; (b) comparison of microdumbbells in air and SBF.

implies that larger specimens are intrinsically weaker than smaller specimens when compared at the same strain rate [23]. At the same loading rate (mm/min), smaller specimens will be likely to induce higher strain rates (%/min). Fig. 3a compares the stress–strain plots of L_SIBS31 and L_SIBS34 micro- and standard dumbbells in air. It can be seen that higher tensile strength and lower elongation at break was measured with the microdumbbells. Our long term experience agrees with this finding. The data verifies the strain rate

Table 3
Tensile tests.

Sample	Conditions	σ (MPa)	ε (%)
L_SIBS31 (m)[a]	Air 24 °C	13.5	450
L_SIBS31 (S)[b]	Air 24 °C	11.3	620
L_SIBS34 (m)	Air 24 °C	16.4	445
L_SIBS34 (S)	Air 24 °C	15.4	598
L_SIBS31 (m)	SBF 24 °C	14.0	440
L_SIBS34 (m)	SBF 24 °C	12.8	430
L_SIBS31 (m)	SBF 37 °C	12.5	585
L_SIBS34 (m)	SBF 37 °C	10.5	512

Average of 5 measurements; typical SD = 0.1 MPa and 20%.
[a] m, microdumbbell.
[b] S, standard dumbbell.

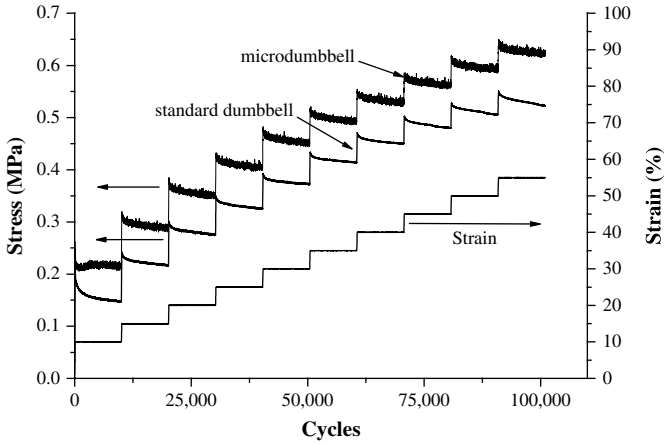

Fig. 4. SIST for L_SIBS31 using standard and microdumbbells in air, $f = 1$ Hz, $T = 24$ °C.

effect discussed above, so microdumbbells can be considered as a "worst case" scenario.

Fig. 3b shows stress–strain plots measured using microdumbbells in SBF at 24 °C and 37 °C. It can be seen that at 37 °C the plots merged, with both polymers demonstrating lower ultimate tensile strength and more elongation. L_SIBS34 showed higher ultimate tensile strength and elongation than L_SIBS31, which is consistent with the higher MW and broader MWD of the former material. The ultimate values are summarized in Table 3. In SBF at 37 °C, L_SIBS34 seems to have lost more strength than L_SIBS31. The Young moduli values remained the same at 2 MPa.

Stepwise Increasing Strain Test (SIST) was also carried out with micro- and standard specimens starting with 10% strain to give stress values that were within the instrument detection capability. Also, 10% strain is the limit under normal physiological conditions (e.g., tendon strain). As discussed in our accompanying paper in this journal [18], testing of soft materials presents special challenges (e.g., load cell size, buckling etc.) which will be further exacerbated by reducing the sample size. During this test, the specimens were exposed to increasing levels of strain, lasting 10,000 cycles each. Fig. 4 presents the strain applied during the SIST, and the stresses obtained at each strain level for L_SIBS31. Standard and microdumbbells followed similar trends, with higher stresses measured with the microdumbbells. This is consistent with the tensile measurements. Since higher stresses accelerate fatigue, we can again conclude that

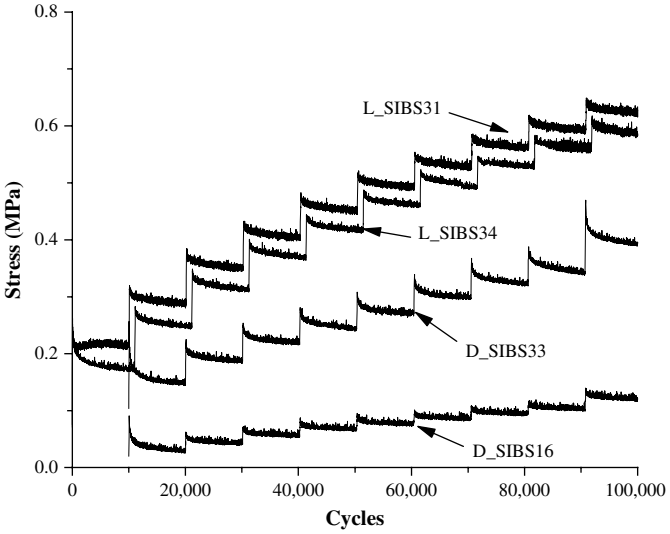

Fig. 5. Stress values during the SIST in air $f = 1$ Hz, $T = 24$ °C.

Table 4
Dynamic relaxation vs strain.

Strain (%)	Stress change (dynamic relaxation) (%)			
	L_SIBS31	L_SIBS34	D_SIBS33	D_SIBS16
10	15	26	–	–
15	9	11	15	20
20	8	11	10	9
25	7	8	13	15
30	6	5	11	14
35	6	6	11	7
40	4	6	12	13
45	5	3	12	13
50	5	2	16	11
55	5	6	16	10

testing microdumbbells present the "worst case" scenario. Based on this, further testing was performed with microdumbbells only.

3.2. Fatigue testing

3.2.1. SIST

Stepwise Increasing Strain Test (SIST) under strain-controlled conditions was used to determine the fatigue limit of the different samples. The stress values at each step, shown in Fig. 5, give an indication of the instantaneous change in tensile strength (here attributed to dynamic relaxation) due to deformation. The strain was increased from 10% to 55% during the test. L_SIBS34 had somewhat lower stresses than L_SIBS31. D_SIBS33 displays a less steep slope than the linear samples, with D_SIBS16 showing the lowest stresses and the most gradual change. The presence of branching in the dendritic samples led to better stability under cyclic loading.

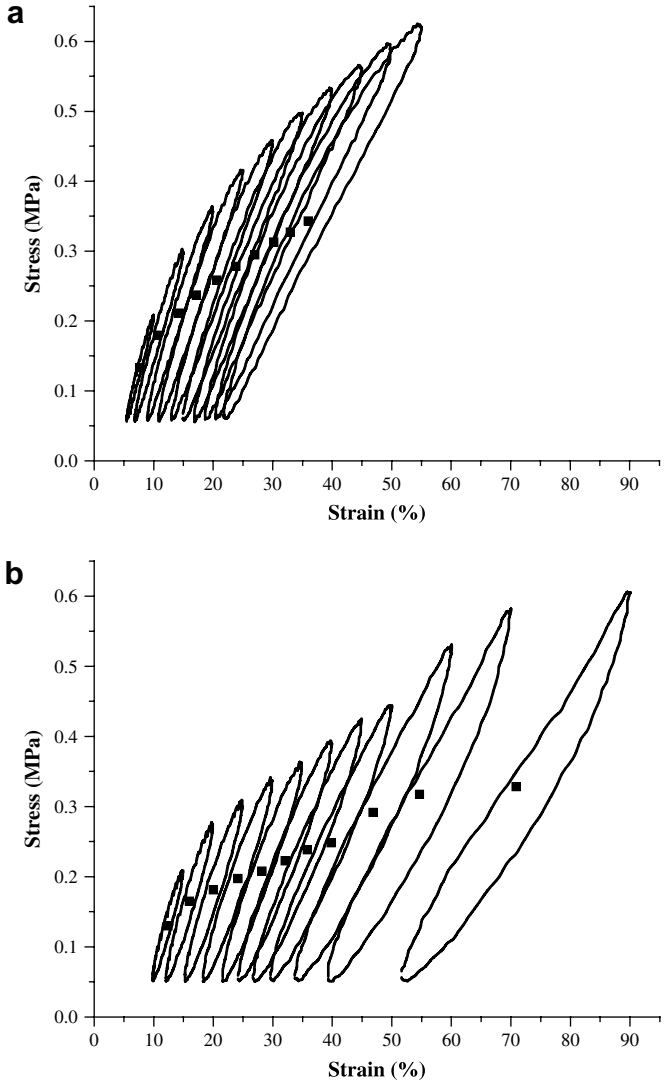

Fig. 6. Hysteresis loops of (a) L_SIBS31 and (b) D_SIBS33. SIST, $f = 1$ Hz and $T = 24$ °C.

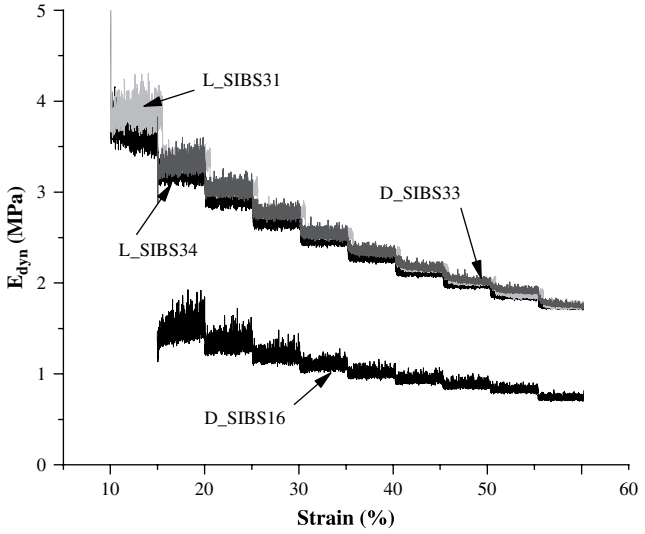

Fig. 7. Dynamic moduli profiles in air at 24 °C. $f = 1$ Hz.

The decrease in stress (stress relaxation) in each 10,000 cycle step, obtained from Fig. 5, is shown in Table 4. The dendritic samples show greater stress relaxation. This can be explained with the branched PIB core in the dendritic samples. D_SIBS16 displayed stress relaxation in the same range as D_SIBS33, in spite of its lower PS content and less branching, which is most likely due to the higher MW (more entanglements) and higher rubbery phase content.

Since the testing method adopted for small and soft specimens is new, we could not find comparative data in the literature. The effect of branching on fatigue properties of polymers has mostly been investigated using crack propagation. For example, the fatigue properties in polyethylene were shown to improve with branching, but the effects of branching and MWD were difficult to separate [27]. Broad/bimodal MWD (the presence of high MW fractions)

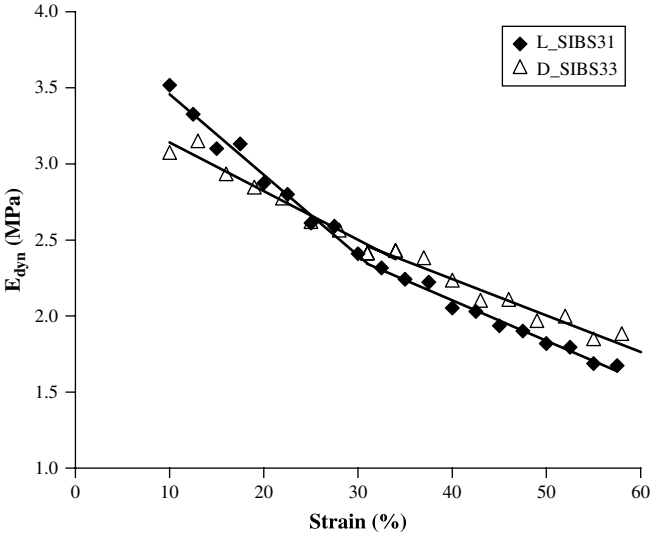

Fig. 8. Average dynamic moduli vs. strain plots for L_SIBS31 and D_SIBS33 constructed from Fig. 7.

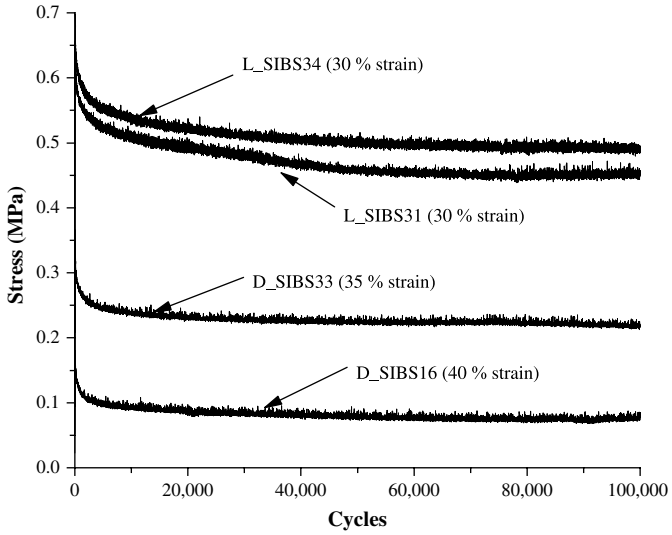

Fig. 9. Stresses measured with the fatigue limit strains (30, 35 and 40%). 100,000 cycles, $f = 1$ Hz, air at $T = 24\,^{\circ}C$.

improved the fatigue properties of polyurethane [28]. Branched butyl rubber also showed improved fatigue properties [29,30]. The stress relaxation of branched PIBs with narrow and broad MWD and linear PIBs has been investigated [8,31]. It was found that regardless of the MWD there was a correlation between the "instantaneous" recovery and the MW; the sample with the lowest MW recovered in the shortest time. Comparison of samples with similar $M_w \sim 10^6$ g/mol but narrow and multimodal/broad MWD revealed that the former relaxed much faster. Based on the limited information available, it can be concluded that higher MW and broader MWD will have a beneficial effect on fatigue life. The present findings are in line with this general trend.

The evolution of the hysteresis loops of L_SIBS31 and D_SIBS33 is shown in Fig. 6. It can be observed that the areas of the loops with the same maximum strain are noticeably smaller for the D_SIBS33 copolymer. It was reported [17] that the occurrence of the fatigue limit corresponds to the leveling off of the midpoint stresses, which are marked in the plots. In Fig. 6, no leveling off was observed up to 50–55% strain. D_SIBS33 was tested up to 90% strain and it was seen that above 60% strain the hysteresis curves became noticeably deformed (Fig. 6b). "Pinching" in the hysteresis loop is an indication of permanent damage or deformation. Visual observation confirmed that above 60%, physical damage occurred on the surface of the samples. Because this method was not sensitive enough to determine the fatigue limit, the dynamic moduli (i.e., the slope of the hysteresis loops) were used instead. The dynamic moduli (E_{dyn}) vs. strain plots calculated from the hysteresis loops below 60% strain are shown in Fig. 7. The samples with ~30 wt% PS show similar profiles, while the E_{dyn} of D_SIBS16 is considerably lower at each strain level.

Fig. 8 shows the average E_{dyn} at each strain level vs. strain plot for L_SIBS31 and D_SIBS33. The change in the slope of the line indicates that permanent, irreversible deformation has occurred,

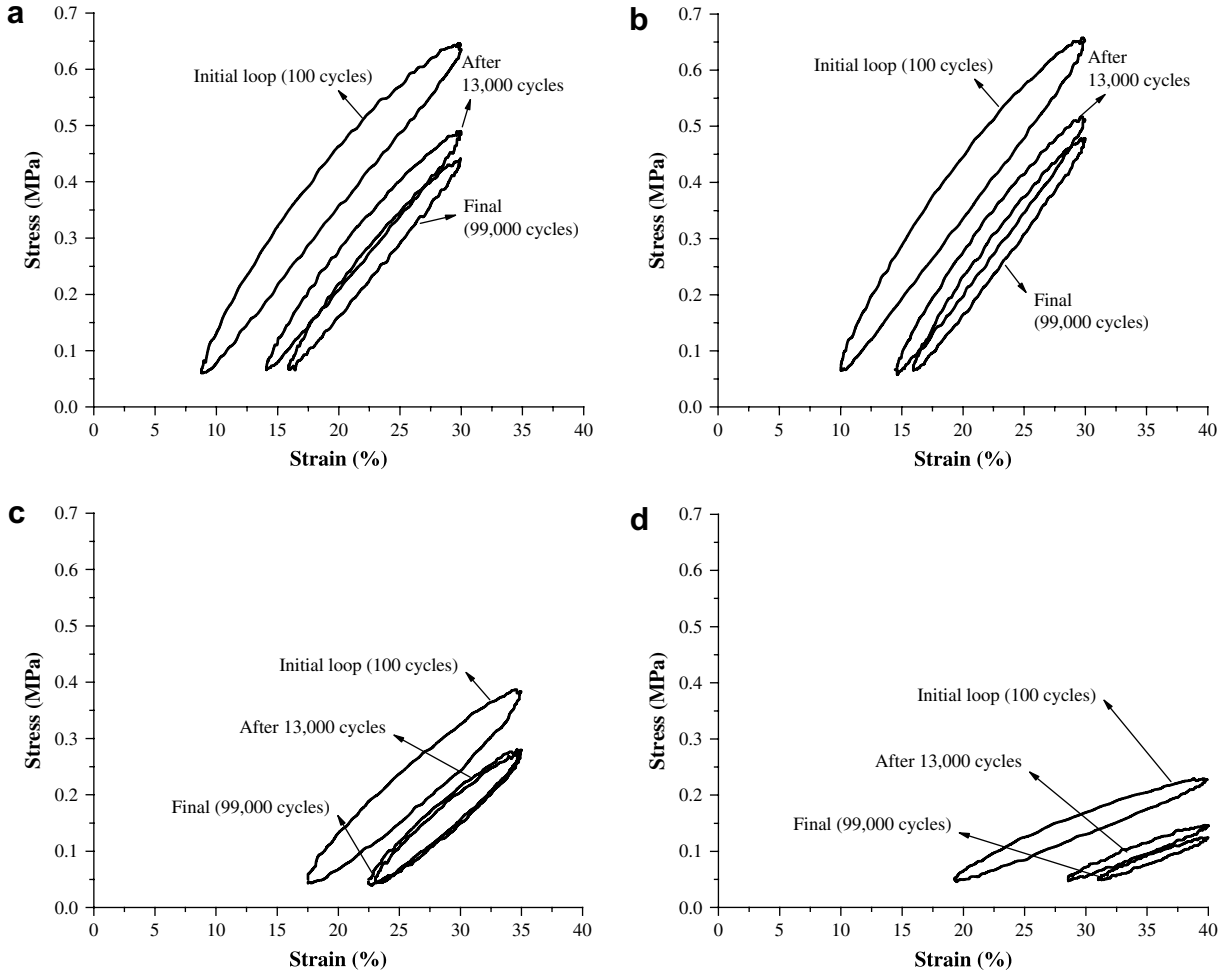

Fig. 10. Hysteresis loops evolution at the fatigue limit strains (100,000 cycles, $f = 1$ Hz, $T = 24\,^{\circ}C$). (a) L_SIBS31 – 30%, (b) L_SIBS34 – 30%, (c) D_SIBS33 – 35%, (d) D_SIBS16 – 40%.

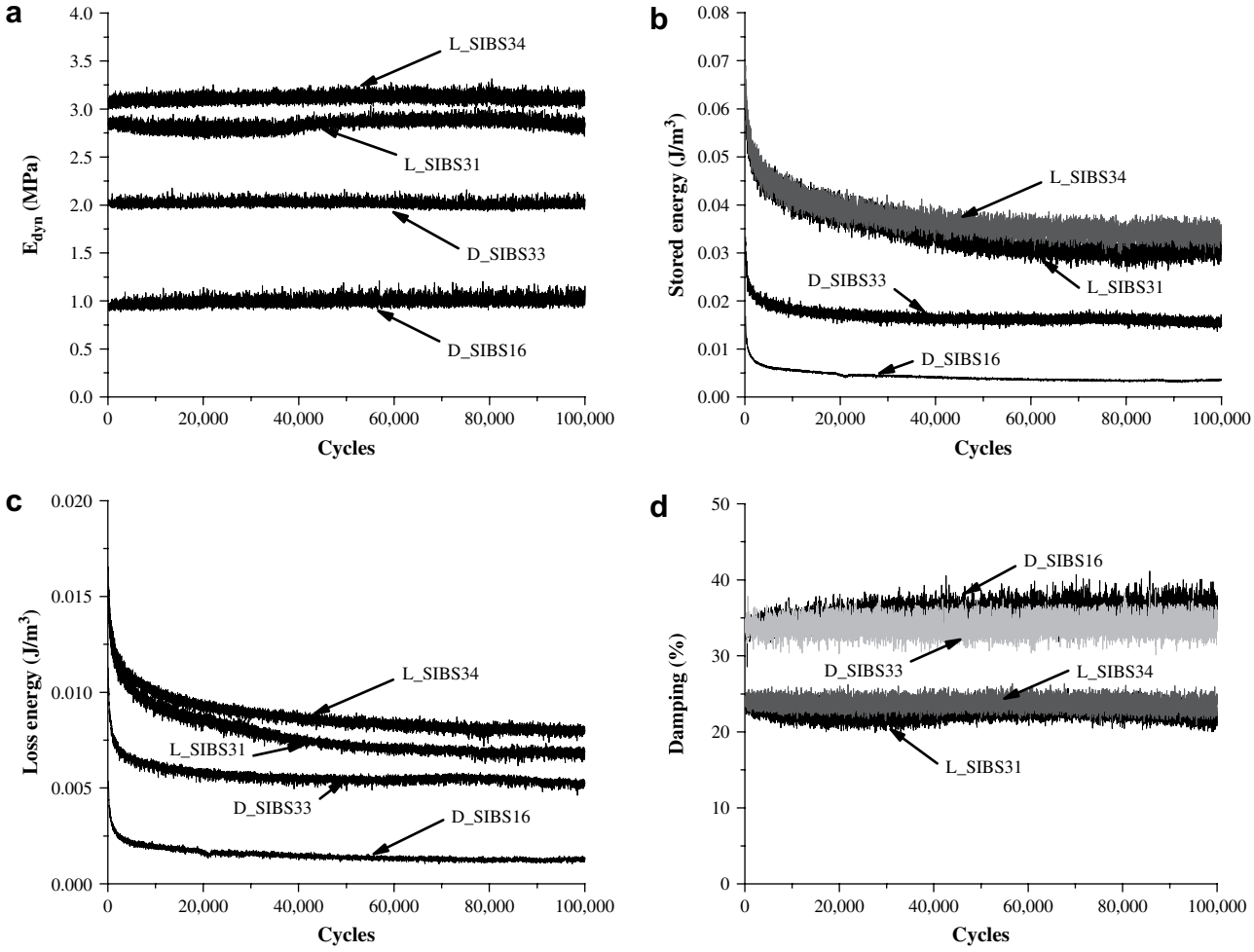

Fig. 11. (a) Dynamic moduli, (b) stored energy, (c) loss energy and (d) damping profiles. 100,000 cycles, $f = 1$ Hz, $T = 24$ °C.

causing a loss in material stiffness [15,32]. The strain at which this change takes place is associated with the fatigue limit, which was 30% strain for both of the linear samples, and 35 and 40% for D_SIBS33 and D_SIBS16, respectively. D_SIBS33, whose PS content is similar to that of the linear samples, is expected to have a higher fatigue limit (defined as the maximum strain before the dynamic modulus becomes unstable, i.e. changes more than 5%), due to the branching in the rubbery phase. Indeed, smaller drops in the dynamic modulus at the same strain level were observed for D_SIBS33. Surprisingly, D_SIBS16 with much lower PS content exhibited a higher fatigue limit than D_SIBS33, most likely due to its higher MW (although somewhat less branched) PIB core.

3.2.2. Long term testing (100,000 cycles)

Long term testing in air at 24 °C at the fatigue strain limit measured as discussed above provides an effective comparison between polymers, while representing the worst case scenario in terms of conditions that can be experienced by the polymers. Fig. 9 presents the stresses experienced by each polymer over the course of 100,000 cycles at its own fatigue strain limit (30, 30, 35 and 40%). D_SIBS33 had much lower stresses than L_SIBS31 and L_SIBS34, in spite of its similar PS content. This can be attributed to the ordered microdomain structure of the linear polymers, in comparison with the disrupted microdomains in D_SIBS33 shown earlier by AFM [33]. D_SIBS16 has the lowest stresses, on account of its lowest PS content and highest PIB MW. Fig. 10 shows the hysteresis loop evolution for the polymers. The loops of L_SIBS31 and L_SIBS34 shifted towards lower stress levels over the entire experiment, while the D_SIBS33 loops shifted only during the first 13,000 cycles, after which they stayed relatively constant. This indicates better shape retention in the dendritic polymer. The loops of D_SIBS16 also shifted throughout the experiment, translating into less shape retention due to the lower PS content. The larger hysteresis loops of the linear samples relative to the dendritic samples indicate more pronounced fatigue in the former.

The dynamic modulus, stored and loss energy and damping are shown in Fig. 11. The dynamic moduli (Fig. 11a) of the materials did not change appreciably with time. This fact provides an indication that no permanent internal damage occurred during the long term testing. L_SIBS31 and L_SIBS34 showed marginal differences in terms of physical properties. The slightly higher dynamic moduli of L_SIBS34 are attributed to the higher PS content. However, D_SIBS33 has significantly lower stresses than the linear samples at comparable hard block content; most likely because the absence of ordered and regular phases found in linear block copolymers [34] reduce the strength of this material. As a consequence of this, the dynamic moduli values and stored energies are much lower in D_SIBS33, and its damping is much higher than that of the linear samples, suggesting improved capability for energy absorption. Even though the more irregular/distorted hard phases seen by AFM [33] may sacrifice mechanical strength, the *arborescent* structure of the PIB phase results in increased ability to dissipate energy. Furthermore, when examining D_SIBS16 in comparison with D_SIBS33, the lower PS content, higher rubbery block content and

molecular weight in the former produce a more compliant material, with lower energy values and higher damping.

3.2.3. Fatigue testing under simulated physiological conditions

Preliminary experiments revealed that hydrostatic pressure and fluid shear forces on the load cell became a major issue when attempting to conduct fatigue tests with microdumbbells using the chamber loaded with SBF [16]. Specifically, pumping of the SBF caused a disturbance in data collection, which was very significant, since the signals obtained were close to the sensitivity limit of the load cell. Controlling the minimum strain at 20% still yielded quite a high noise so the results can only be considered as orienting values. The first 12,000 cycles in air at 24 °C yielded similar constant E_{dyn} profiles than those in Fig. 11a. Upon addition of SBF at 37 °C, no appreciable changes were observed. We are working on increasing the sensitivity of our equipment to investigate the effects of SBF in more detail.

4. Conclusions

We developed a dynamic fatigue testing methodology for small, soft rubbery specimens (microdumbbells) that can be implanted into small animals and re-tested after explantation. Higher ultimate tensile strength and lower elongation at break were measured on microdumbbells than on standard dumbbells. In fatigue testing microdumbbells induced higher stresses at the same strain rate, thus present the worst case scenario and are appropriate for fatigue tests.

The fatigue limit was determined using SIST. The presence of branching and broader molecular weight distribution in D_SIBS led to better stability and higher fatigue limit than in linear SIBS samples. Long term testing in air at 24 °C conducted at the fatigue limit showed that no permanent internal damage occurred during the tests. D_SIBS16 with high molecular weight and relatively low PS content showed better fatigue properties than D_SIBS33 and linear SIBS31 and SIBS34. Preliminary data indicated that simulated physiological conditions would have a negligible effect on the dynamic modulus and stress relaxation behavior. The method developed here for small specimens is a promising technique to test new biomaterials.

Acknowledgement

This material is based upon work supported by the National Science Foundation under DMR-0509687 the Deutsche Forschungsgemeinschaft DFG under AL 474/12-1 and the Polish Ministry of Science. The authors acknowledge the contribution of Dr. Goy Teck Lim to this work.

References

[1] Kaszas G, Puskas JE, Hager W, Kennedy JP. US Patent 4,946,897; 1990.
[2] Kaszas G, Puskas JE, Hager W, Kennedy JP. J Polym Sci Part A Polym Chem 1991;29(3):427–35.
[3] Puskas JE, Kaszas G. Rubber Chem Technol 1996;69(3):462–75.
[4] Puskas JE, et al. US Patent 6,747,098; 2004.
[5] Publication PO30025 U.S. Food and Drug Administration. Taxus express2™ paclitaxel-eluting coronary stent system (monorail and over the wire). Washington, DC: U.S. Government Printing Office; 2004.
[6] Pinchuk L, Wilson GJ, Barry JJ, Schoephoerster RT, Parel J-M, Kennedy JP. Biomaterials 2008;29(4):448–60.
[7] El Fray M, Prowans P, Puskas JE, Altstädt V. Biomacromolecules 2006;7(3):844–50.
[8] Puskas JE, Paulo C, Altstädt V. Rubber Chem Technol 2002;75(5):853–63.
[9] Puskas JE. Polym Prepr 2004;45(2):412–3.
[10] Puskas JE, Kaszas G, Dos Santos LM. J Polym Sci Part A Polym Chem 2006;44(21):6494–7.
[11] Sui C, McKenna GB, Puskas JE. J Rheol 2007;51(6):1143–69.
[12] Puskas JE, Dos Santos LM, Sen MY, Kaszas G. Rubber Chem Technol 2007;80(4):661–71.
[13] Puskas JE, Chen Y, Antony P, Kwon Y, Kovar M, Harbottle RR, et al. Polym Adv Technol 2003;14(11–12):763–70.
[14] Puskas JE, Antony P, Kwon Y, Kovar M, Norton PR. J Macromol Sci Macromol Symp 2002;183:191–7.
[15] El Fray M, Altstädt V. Polymer 2003;44(16):4635–42.
[16] El Fray M, Altstädt V. Polymer 2003;44(16):4643–50.
[17] El Fray M, Altstädt V. Polymer 2004;45(1):263–73.
[18] Puskas JE, El Fray M, Tomkins M, Dos Santos LM, Fischer F, Altstädt V. Polymer, submitted for publication.
[19] Puskas JE, Kwon Y. Polym Adv Technol 2006;17(9–10):615–20.
[20] Renke-Gluszko M, El Fray M. Biomaterials 2004;25(21):5191–8.
[21] Cahoon JR, Holte RN. J Biomed Mater Res 1981;15(2):137–45.
[22] Cho SB, Miyaji F, Kokubo T, Nakamura T. J Mater Sci Mater Med 1998;9(5):279–84.
[23] Griffith A. Philos Trans R Soc London Ser A 1921;221:163–98.
[24] Kase S. J Polym Sci 1953;11(5):425–31.
[25] Odom EM, Adams DF. J Mater Sci 1992;27(7):1767–71.
[26] Weibull W. J Appl Mech T ASME 1951;18(3):293–7.
[27] Shah A, Stepanov EV, Capaccio G, Hiltner A, Baer E. J Polym Sci Part B Polym Phys 1998;36(13):2355–69.
[28] Kaneko Y, Watabe Y, Okamoto T, Iseda Y, Matsunaga T. J Appl Polym Sci 1980;25(11):2467–78.
[29] Duvdevani I, Powers KW, Wang H-C. PMSE 1997;77:101–2.
[30] Kaszas G. Rubber Expo 2001, Fall Technical Program, 160th, Cleveland, OH, United States, Oct. 16–20, 2001; p. 1514–35.
[31] Robertson CG, Roland CM, Puskas JE. J Rheol 2002;46(1):307–21.
[32] Orth F, Hoffmann L, Zilch-Bremer H, Ehrenstein GW. Compos Struct 1993;24:265–72.
[33] Antony P, Kwon Y, Puskas JE, Kovar M, Norton P. Eur Polym J 2003;40(1):149–57.
[34] Ritchie RO, Dauskardt RH, Yu W, Brendzel AM. J Biomed Mater Res 1990;24(2):189–206.